Research Square

Preprints are preliminary reports that have not undergone peer review.
They should not be considered conclusive, used to inform clinical practice,
or referenced by the media as validated information.

Modeling and multi-objective optimization of electrocoagulation operating parameters for urban wastewater treatment

Sarra Hamidoud

sarrahamidoud24@gmail.com

8 May 1945 Guelma university

Research Article

Keywords: Wastewater Treatment, Green Process, Electrocoagulation, Experimental Design, Modelling, Optimization.

Posted Date: August 11th, 2026

DOI: https://doi.org/10.21203/rs.3.rs-10392528/v1

License: This work is licensed under a Creative Commons Attribution 4.0 International License.
Read Full License

Additional Declarations: No competing interests reported.

Version of Record: A version of this preprint was published at Water Conservation Science and Engineering on September 9th, 2026. See the published version at https://doi.org/10.1007/s41101-026-00563-4.

Modeling and multi-objective optimization of electrocoagulation operating parameters for urban wastewater treatment

Sarra Hamidoud [a*]

[a] Materials Engineering and Industrial Analysis Laboratory (M.E.I.A.L.), University 8 May 1945 Guelma, Algeria, P.O 401 Guelma 2400.

[*] Corresponding author: sarrahamidoud24@gmail.com

Abstract

In this study, the electrocoagulation (EC) process that uses electric current to remove contaminants from water, was used to optimize the treatment of urban wastewater. This process is an alternative treatment method that has attracted increasing attention, which are often limited by high costs and significant sludge production. The study aimed to optimize the turbidity (cloudiness caused by suspended particles) and chemical oxygen demand (COD, which measures organic pollutant levels) using response surface methodology combined with a central composite design.

The experiment was conducted using real effluent from a wastewater treatment plant. The initial COD was 386.70 mg/L and the turbidity was 202.29 NTU. Four key parameters were studied: current intensity (X_1), electrode surface area (X_2), electrolysis time (X_3), and stirring speed (X_4). This process relies on the dissolution of sacrificial iron anodes. This generates metal hydroxides that destabilize pollutants via charge neutralization and adsorption.

Variance analysis showed an excellent fit of the mathematical models, with high coefficients of determination (R^2 = 97.72 for turbidity and 99.25 for COD). The current intensity was the most influential factor for both responses. Turbidity removal followed a nearly linear behavior. However, COD removal exhibited significant quadratic effects (p = 0.004), indicating more complex interaction mechanisms, such as adsorption and oxidation, and the existence of an internal optimum.

Multi-objective optimization enabled the identification of ideal operating conditions: a current intensity of 0.775 A, an electrode surface area of 375 cm^2, a time of 75 min, and agitation at 400 rpm. Under these conditions, the study achieved near-total turbidity removal (~100%) and a COD reduction of 97.57%. This study confirms that RSM-optimized electrocoagulation constitutes a highly effective solution for the purification of domestic effluents, paving the way for more sustainable industrial applications.

Keywords

Wastewater Treatment, Green Process, Electrocoagulation, Experimental Design, Modelling, Optimization.

Abbreviations

E.C: Electrocoagulation

COD: Chemical Oxygen Demand

ANOVA: Analysis of variance

RSM: Response surface methodology

CCD: Central composite design

1. Introduction

Water resource pollution is one of the main environmental challenges today, owing to the continuous increase in industrial and domestic wastewater discharges (Yusmaini et al., 2023). These effluents typically contain suspended solids, organic compounds (Mokhter, 2017), and colloidal substances responsible for high turbidity and a high chemical oxygen demand (COD) (Osman, 2022), thereby affecting the quality of the receiving environments and the health of aquatic ecosystems (Natchia et al., 2023).

Conventional wastewater treatment processes, such as chemical coagulation-flocculation, adsorption, and biological treatments, have several limitations, including reduced effectiveness for certain pollutants, significant sludge production, and high operating costs (Nabbou et al., 2025). These constraints have led to a growing interest in the development of alternative technologies that are more efficient and environmentally friendly (Bellebia et al.,2009) (Shamshad & Rehman, 2025).

Among these technologies, electrocoagulation has proven to be a promising method for the removal of pollutants present in wastewater, such as turbidity (Zodi, 2012), organic matter (Garcia-Segura et al., 2017), and heavy metals (Al-Shannag et al., 2015) (Bazrafshan et al.,2015). It has been successfully applied in the treatment of textile effluents containing dyes (Bayramoglu et al.,2004) (Núñez et al.,2019), agri-food wastewater rich in organic matter (Zongo, 2009), and industrial effluents (İrdemez et al.,2006) (Asselin, 2007) contaminated by heavy metals such as lead (Fu-Hu, 2015) and chromium (Kamar et al.,2018) (Adhoum et al.,2004). This electrochemical process relies on the anodic dissolution of sacrificial electrodes, typically made of aluminum or iron, enabling the in-situ generation of coagulant species capable of neutralizing surface charges and promoting the aggregation of colloidal particles (Moussa et al.,2017). In the case of iron electrodes, the anode dissolves under the effect of the electric current according to the following oxidation reaction:

$Fe \rightarrow Fe^{2+} + 2\bar{e}$ (1)

The ferrous ions formed can then be oxidized into ferric ions:

$Fe^{2+} \rightarrow Fe^{3+} + \bar{e}$ (2)

At the cathode, the reduction of water leads to the formation of hydrogen and hydroxide ions:

$2H_2O + 2e^- \rightarrow H_2 + 2OH^-$ (3)

The generated metal ions then react with the hydroxide ions present in the solution to form metal hydroxides, such as $Fe(OH)_2$ and $Fe(OH)_3$. These species possess strong coagulating power, enabling the destabilization of colloidal particles and the adsorption of pollutants present in the effluent, leading to the formation of easily separable flocs (Bennajah, 2007).

Pollutant Removal Mechanisms

The removal of contaminants during electrocoagulation primarily relies on several mechanisms:

- The neutralization of colloidal particle charges,
- The adsorption of pollutants onto the formed metal hydroxides,
- Sweep flocculation,

These mechanisms lead to the aggregation of particles and their removal through sedimentation or flotation (Fouad et al.,2009) (Zaied et al., 2020).

Numerous studies have demonstrated the effectiveness of electrocoagulation in reducing turbidity and COD, with the advantage of reducing the use of chemical reagents (Ebba et al., 2022).

However, the efficiency of the electrocoagulation process depends heavily on operational parameters such as current intensity, electrode surface area, electrolysis time, and agitation. The simultaneous optimization of these parameters remains a challenge, particularly when multiple responses must be maximized simultaneously. In this context, the application of the response surface methodology (Response Surface Methodology, RSM) combined with an experimental.

Design constitutes a powerful statistical tool for analyzing the individual and interactive effects of operational factors and determining the optimal process conditions (Asaithambi et al., 2018).

The primary objective of this study was to optimize wastewater treatment through electrocoagulation by simultaneously maximizing turbidity and COD removal efficiencies using a multi-objective optimization approach based on RSM. This study also aims to better understand the influence of operational parameters and their interactions to improve process performance and contribute to its industrial-scale application.

This methodology provides a comprehensive understanding of the electrocoagulation process that would be impossible to achieve through traditional experimental methods, while also delivering optimal conditions directly applicable at an industrial scale.

2. Experimental and methods

2.1 Influence of operational parameters

A. Current intensity

The current intensity controls the electrode dissolution rate and the production of metallic ions. Increasing the current promotes the formation of coagulating hydroxides and generally improves the pollutant removal efficiency (Dubrawski et al.,2014) (Nasrullah et al., 2019).

B. Electrode Surface

The electrode surface area influences the active zone available for electrochemical reactions to occur. A larger surface area allows for greater metal ion production and improves process performance (Wu et al., 2022).

Electrolysis Time

The electrolysis time determines the total amount of coagulant generated in the system. A longer time promotes pollutant removal but can increase energy consumption (Ibrahim and Salman, 2022).

C. Stirring Speed

Stirring enhances mass transfer within the reactor and promotes contact between pollutants and metal hydroxides, which improves floc formation (Trinh et al.,2021).

2.2 Statistical Analysis

Several factors can influence an electrochemical reaction, including the nature and type of electrode used, the composition and nature of the solution, and the environmental conditions (Khemis, 2005). According to our comprehensive literature review and parameter screening, the applied current, treatment time, contact surface area, and magnetic stirring were the most influential parameters. The ranges and levels chosen for these variables were based on a synthesis of previous studies in the literature and were supported by preliminary experiments conducted in our laboratory to ensure their relevance for the type of urban wastewater and reactor size used in this study. The selection of the levels for the studied variables is presented in the following table.

Table 1: Experimental parameter variation domains and levels studied.

Parameters	Current Density (A)	Contact Area (cm^2)	Electrolysis Time (min)	Magnetic Stirring (rpm)
Variables and Concept	X_1	X_2	X_3	X_4
Low Level (-1)	0.25	150	30	100
Mid-Level (0)	0.425	225	45	200
High Level (-1)	0.6	300	60	300

2.3. Experimental Design (DOE)

The response surface methodology (RSM) was applied using a central composite design (CCD) (AlJaberi,2023). The implementation of the CCD is essential to achieve the rotatability of the linear and quadratic terms, offering significant advantages for the optimization and exploration of interrelationships between several independent variables and one or more dependent variables (Bhattacharya, 2021).

This statistical approach allows the establishment of a mathematical model describing the relationship between the operational variables and the system responses.

The experimental design was structured to study the influences of four main factors: current intensity, electrolysis time, electrode surface area, and agitation, while the analyzed responses were the turbidity removal yield and COD. Multi-objective optimization was performed using the desirability function, which transforms multiple responses into a global function to be maximized to determine the optimal operating conditions. This approach not only improves the overall efficiency of the electrocoagulation process but also enhances the understanding of the influence and interactions of the operating parameters on the treatment performance (Trigueros et al., 2022).

The yield expressions were given by the variation in turbidity and COD of the wastewater under the effect of an electric current, relative to the initial turbidity and COD according to the following relationship:

$$\boldsymbol{\eta}(\%) = \left(\frac{\text{Turbidity}_{\text{i}} - \text{Turbidity}_{\text{f}}}{\text{Turbidity}_{\text{i}}}\right).100 \qquad (4)$$

η: Yield (%), **Turbidity$_i$**: Initial concentration of turbidity (mg O_2/l), **Turbidity$_f$:** Final concentration of turbidity (mg O_2/l)

$$\boldsymbol{\eta}(\%) = \left(\frac{COD_i - COD_f}{COD_i}\right).100 \qquad (5)$$

η: Yield (%), **COD_i:** Initial concentration of Chemical Oxygen Demand (mg O_2/l), **COD_f:** Final concentration of chemical oxygen demand (mg O_2/l).

All experiments used a combination of parameters and levels (As shown Table 2).

Table 2 : Experiment design matrix.

Variable experiment	**X_1 (A)**	**X_2(cm^2)**	**X_3(min)**	**X_4(rpm)**	**Y_1(%)**	**Y_2(%)**
1	1	-1	0	0	93.34	88.90
2	0	-1	-1	0	90.19	85.90
3	-1	-1	0	0	89.36	84.15
4	1	0	0	-1	95.53	90.98
5	0	-1	0	1	93.71	89.25
6	0	1	0	-1	90.55	86.24
7	1	0	0	1	94	89.53
8	0	0	0	0	91.51	87.16
9	0	0	-1	-1	89.23	84.98
10	-1	0	-1	0	89.10	84.70
11	1	0	-1	0	91.57	87.21
12	0	-1	1	0	89.83	85.56
13	1	1	0	0	94.39	89.89
14	0	-1	0	-1	91.15	86.74
15	0	1	-1	0	93.52	89.07
16	0	1	1	0	91.75	87.38
17	0	0	1	-1	89.33	85.08
18	-1	0	0	-1	90.19	85.90
19	0	0	-1	1	92.92	88.50
20	-1	0	1	0	92.81	88.39
21	0	0	0	0	91.50	87.11
22	0	0	0	0	91.57	87.18
23	0	0	1	1	90.38	86.08
24	0	1	0	1	92.97	88.55

25	-1	0	0	1	88.32	84.11
26	1	0	1	0	96.02	91.44
27	-1	1	0	0	91.75	87.38
28	0	0	0	0	90.41	86.5
29	0	0	0	0	90.35	85.9
30	0	-1	0	1	92.06	88.3
31	0	1	-1	0	89.6	85.8

2.4. Studied Effluent

The raw effluent used in this study was collected from the inlet of the Guelma City wastewater treatment plant (WWTP). Urban-origin samples were collected in previously cleaned polyethylene bottles and stored at 4°C to stabilize their physicochemical properties and inhibit any biological activity prior to experimental testing.

2.5. Experimental Setup

Electrocoagulation experiments were conducted in a rectangular glass reactor with a volume of 500 ml. The electrochemical system comprised six rectangular iron electrodes arranged in a parallel configuration. Each electrode measured 7.5 cm in length, 5 cm in width, and 0.1 cm in thickness, corresponding to a total active surface area of 225 cm^2. The electrodes were connected to a DC power supply (Metrix AX501) to allow precise control of the applied current intensity.

The interelectrode distance was kept constant throughout the tests to ensure a homogeneous distribution of the electric field. Magnetic stirring was performed using a variable-speed magnetic stirrer to promote the mass transfer and homogenization of the suspension. Before each experiment, the electrodes were washed with an acetone solution to remove all prior impurities and ensure reproducibility of the operating conditions as shows in Fig.1. The tests were conducted in batch mode according to the conditions defined in the experimental plan.



Figure 1: Experimental setup of the EC assembly.

3.Results and discussion

3.1. Wastewater Characterization

As shown in Table 1, the urban wastewater exhibited distinct physicochemical parameters. The average pH of the laundry greywater presented in Table 3 was 7.52, which is close to neutral. Iron electrocoagulation is a suitable technology for treating laundry greywater, as the optimal pH range for iron electrocoagulation is typically between 6.0 and 8.0. Within this range, iron electrodes are most effective for generating iron hydroxide flocs, facilitating contaminant removal.

The main characteristics of the raw effluent, including pH, turbidity, and chemical oxygen demand (COD), were measured using standard methods before each experiment and are presented in the following table:

Table 3 : Wastewater characteristics.

Parameter	Average Value	Maximum
pH	7.52	7.8
Temperature (°C)	15.42	18.2
Conductivity (µS/cm)	1.398	1.8
COD (mg O_2/L)	386.70	488

BOD_5 (mg O_2/L)	215	284.4
TSS (mg/L)	278.7	300
Turbidity (NTU)	202.29	550
NO_3^- (mg/L)	4.22	6.5
NO2- (mg/L)	4.46	5.8

3.2. Construction of the Mathematical Model

The experimental data obtained from the experimental design were analyzed using response surface methodology to establish a mathematical model describing the relationship between the independent variables and the studied response (Mäkelä, 2017).

The second-order polynomial model used in the response analysis is expressed by the following equation:

$$Y = a_0 + \sum_{i=1}^{m} a_i X_i + \sum_{ij=1}^{m} a_{ij} X_{ij} + \sum_{ijk=1}^{m} a_{ijk} X_{ijk} + \sum_{i=1}^{m} a_{ii} X_i^2 \qquad (6)$$

Where:

Y represents the response function (turbidity or COD),

a_0 is the model constant,

a_i are the coefficients of the linear effects,

a_{ij} represents the coefficients of the interactions between the variables, aii corresponds to the coefficients of the quadratic effects,

X_i and X_j are the coded independent variables, and m represents the number of factors studied (Talhi, 2010).

In this study, four operational parameters were considered:

X_1: current intensity

X_2: electrode surface area

X_3: electrolysis time

X_4: Agitation speed

The form of this equation for four parameters is as follows:

$$Y = a_0 + a_1X_1 + a_2X_2 + a_3X_3 + a_4X_4 + a_{12}X_1X_2 + a_{13}X_1X_3 + a_{14}X_1X_4 + a_{23}X_2X_3 + a_{24}X_2X_4 + a_{34}X_3X_4 + a_{123}X_1X_2X_3 + a_{124}X_1X_2X_4 + a_{234}X_2X_3X_4 + a_{1234}X_1X_2X_3X_4 + a_{11}x_1^2 + a_{22}X_2^2 + a_{33}X_3^2 + a_{44}X_4^2 \qquad (7)$$

Y refers to the studied responses, namely Y1 and Y2, the turbidity and COD reduction efficiencies expressed as percentages (%).

Table 4: Definition of the influencing factors and responses of the experimental design.

X	X_1	X_2	X_3	X_4	Y_1	Y_2
Parameter	Current (A)	Contact Area (cm^2)	Electrolysis Time (min)	Stirring Speed (rpm)	Turbidity Removal (Efficiency (%)	Chemical Oxygen Demand Removal Efficiency (%)

3.3. Statistical Analysis

Analysis of Variance (ANOVA) is the central statistical tool used in these sources to validate the modeling and prioritize the parameters influencing the treatment efficiency of wastewater by electrocoagulation (Obi et al., 2022). This confirmed the robustness of the mathematical models and distinguished the removal mechanisms for turbidity (Y1) and COD (Y2).

3.4.1. Influence of Operating Parameters on Turbidity Yield

ANOVA confirmed that the quadratic model for turbidity was highly significant, with a p-value < 0.001.

- Model adequacy: The coefficient of determination is R^2 = 97.72%, indicating that the model explained almost all the variability in the experimental data.
- Influential factors: All linear factors (X_1, X_2, X_3, X_4) were significant ($p<0.05$). Current (X_1) was identified as the most dominant factor, with an F-value of 387.37.
- Interactions and curvature: Only the interaction between current and time (X_1X_3) was significant (p=0.003). The absence of significant quadratic terms (p=0.375) demonstrates that the turbidity yield follows an almost linear behavior.

Table 5: Regression parameters and determination coefficients for turbidity yield.

S	R-sq	R-sq (adj)	R-sq (pred)
0.399916	97.72%	95.72%	92.67%

The ANOVA shows that the order of influence of the factors is as follows:

- Current (X_1): This was the dominant factor with the highest F-value (387.37) and a p=0.000. Its

  An Increase enhances the production of ferrous and ferric coagulating agents.
- Electrode surface area (X_2): The second most influential factor (F = 155.87).
- Electrolysis time (X_3): (F = 101.31).
- Current-Time interaction (X_1X_3): This is the only significant interaction (p=0.003), indicating

a synergy for floc maturation.

The quadratic effects were not significant for turbidity, indicating linear behavior.

Table 6: Analysis of Variance (ANOVA) Results for the Response Surface Model of Turbidity.

Source	DF	Adj SS	Adj MS	F-value	P- value
Model	14	109.626	7.8304	48.96	0.000
Linear	4	105.983	26.4958	165.67	0.000
X_1(A)	1	61.953	61.9531	387.37	0.000
X_2(cm^2)	1	24.929	24.9288	155.87	0.000
X_3 (min)	1	16.203	16.2033	101.31	0.000
X_4 (rpm)	1	2.898	2.8982	18.12	0.001
Square	4	0.726	0.1815	1.14	0.375
X_1(A)*X_1(A)	1	0.142	0.1422	0.89	0.360
X_2(cm^2) *X_2(cm^2)	1	0.373	0.3733	2.33	0.146
X_3(min)*X_3(min)	1	0.158	0.1577	0.99	0.336
X_4(rpm)*X_4(rpm)	1	0.268	0.2677	1.67	0.214
Two-Factor Interaction	6	2.917	0.4861	3.04	0.035
X_1(A)*X_2(cm2)	1	0.008	0.0081	0,05	0.825
X_1(A)*X_3(min)	1	2.031	2.0306	12,70	0.003
X_1(A)*X_4(rpm)	1	0.109	0.1089	0,68	0.421
X_2(cm^2) *X_3(min)	1	0.286	0.2862	1.79	0.200
X_2 (cm^2) * X_4 (rpm)	1	0.152	0.1521	0.95	0.344
X_3(min)*X_4(rpm)	1	0.331	0.3306	2.07	0.170
Error	16	2.559	0.1599		
Lack of Fit	10	1.079	0.1079	0.44	0.881
Pure Error	6	1.480	0.2467		
Total	30	112.185			

3.4.2. Influence of parameters on COD removal efficiency

For chemical oxygen demand (COD), ANOVA revealed a more complex structure.

- Model adequacy: The fit was even more precise than that for turbidity, with an R^2 = 99.25%.

- Significance of quadratic terms: Unlike turbidity, the quadratic terms where highly significant (p=0.004). This proves the existence of an internal optimum for the removal of organic matter.
- Key interactions: In addition to the current-time interaction (X_1X_3), the current-agitation interaction (X_1X_4) was significant (p=0.025), highlighting that agitation influences the floc structure and overall efficiency.

Table 7: Regression parameters and coefficients of determination for COD yield.

S	R-sq	R-sq (adj)	R-sq (pred)
0.224210	99.25%	98.60%	96.87%

The influence of factors is more pronounced and complex:

- Current (X_1): was the most dominant factor with a very high F-value of 1177.41.
- Surface (X_2) and Time (X3): with respective F values of 489.03 and 335.86.
- Quadratic terms (X_i^2): Unlike turbidity, they were highly significant (p=0.004), proving the existence of an internal optimum for organic matter removal.
- Significant interactions: X_1X_3 (Current-Time): Highly significant (p=0.000), X_1X_4 (Current-Agitation): Significant (p=0.025), indicating that agitation affects the structure of organic flocs.
- While current intensity is the main driver of treatment in both cases, COD removal is also strongly influenced by curvature (quadratic) effects and more complex interactions between parameters.

Table 8: Analysis of Variance (ANOVA) Results for the Response Surface Model of COD.

Source	DF	Adj SS	Adj MS	F-value	P- value
Model	14	107.147	7.6533	152.24	0.000
Linear	4	104.099	26.0248	517.70	0.000
X_1(A)	1	59.189	59.1890	1177.41	0.000
X_2(cm^2)	1	24.584	24.5835	489.03	0.000
X_3 (min)	1	16.884	16,8840	335.86	0.000
X_4 (rpm)	1	3.443	3.4428	68.49	0.000
Square	4	1.200	0.2999	5.97	0.004

X_1(A)*X_1(A)	1	0.262	0.2621	5.21	0.036
X_2(cm²) *X_2(cm²)	1	0.537	0.5366	10.67	0.005
X_3(min)*X_3(min)	1	0.443	0.4431	8.81	0.009
X_4(rpm)*X_4(rpm)	1	0.327	0.3273	6.51	0.021
Two-Factor Interaction	6	1.848	0.3079	6.13	0.002
X_1(A)*X_2(cm^2)	1	0.104	0.1040	2.07	0.170
X_1(A)*X_3(min)	1	1.249	1.2488	24.84	0.000
X_1(A)*X_4(rpm)	1	0.305	0.3053	6.07	0.025
X_2(cm²) *X_3(min)	1	0.074	0.0743	1.48	0.242
X_2 (cm²) * X_4 (rpm)	1	0.018	0.0176	0.35	0.563
X_3(min)*X_4(rpm)	1	0.098	0.0977	1.94	0.182
Error	16	0.804	0.0503		
Lack of Fit	10	0.520	0.0520	1.10	0.476
Pure Error	6	0.284	0.0474		
Total	30	107.951			

3.5.1. Statistical analysis of Y1 removal efficiency

The Pareto diagram of normalized effects allows identification of statistically significant factors influencing turbidity removal efficiency at the significance threshold a = 0.05 as illustrated in Fig.2.

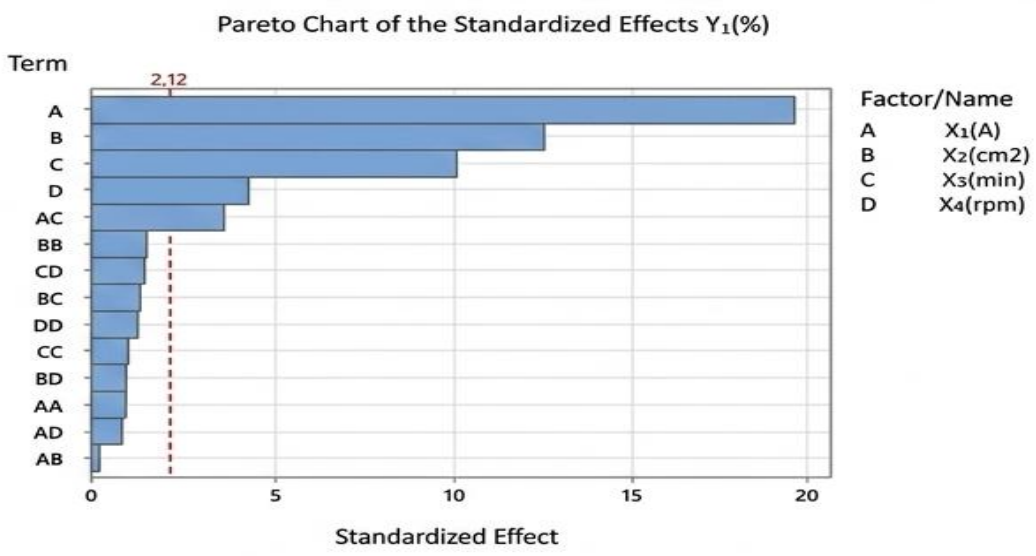


Figure 2: Normalized Effects Pareto Diagram for Response Y1.

The diagram reveals that the current was the most influential factor on turbidity removal, followed by treatment time and their interaction as can be seen in Fig.3. The absence of significant quadratic effects suggests the quasi-linear behavior of the process within the studied experimental domain.

3.5.2. Statistical Analysis of Y_2 Removal Efficiency

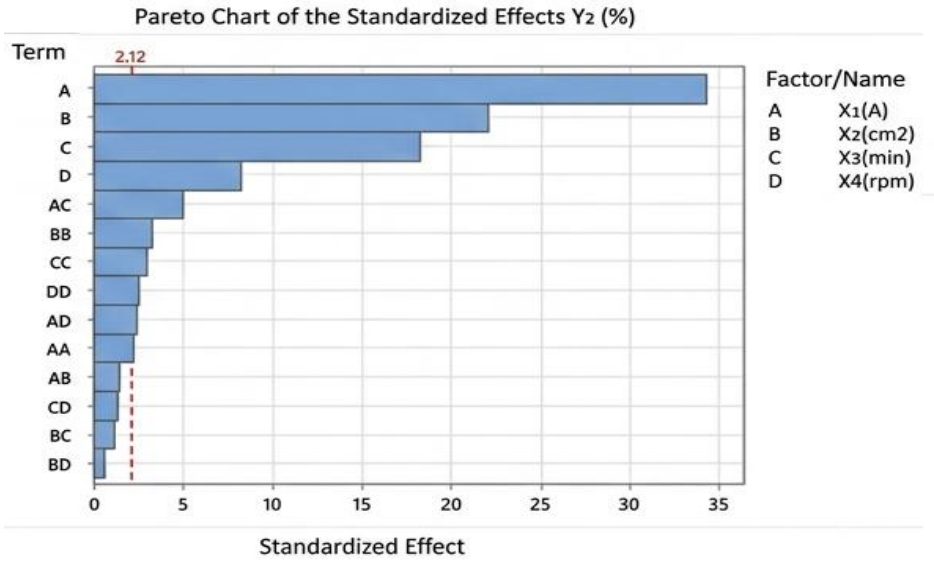


Figure 3: Normalized Pareto chart of effects for response Y2.

The Pareto diagram of the normalized effects shows that factors A (X1), B (X2), C (X3), and D (X4) have a significant influence on the COD removal efficiency, as their effects exceed the significance line (2.12). Factor A had the most dominant effect, followed by B and C. The AC interaction showed a moderate effect, whereas the other interactions and quadratic effects remained non-significant at the 95% confidence level.

Current intensity (X_1) was more influential for COD (Y_2) than for turbidity (Y_1) because of the complexity of the chemical mechanisms involved and the higher statistical sensitivity of COD to this parameter (Mousazadeh et al., 2023).

Here is the evidence extracted from the sources that explains this difference:

1. A clear statistical superiority

The ANOVA performance indicators show that the impact of X_1 is significantly more substantial for COD.

- T-value: For COD, X_1 had a T-value of 34.31, compared to 19.68 for turbidity.
- F Value: The F value for X_1 for COD reaches 1177.41, which is approximately three times higher than that for turbidity (387.37).

This demonstrates that the variation in current explains a much larger proportion of the variance in results for COD than for turbidity.

2. Complexity of Treatment Mechanisms: The increased influence of current on COD is explained by the nature of the pollutants being removed.

- Turbidity: The current primarily generates ferrous/ferric ions for coagulation-flocculation, a relatively direct and linear mechanism.
- For COD: In addition to coagulation, the removal of organic matter (COD) requires more energy-intensive and complex mechanisms, such as adsorption, coprecipitation, and potentially direct or indirect oxidation. X_1 is the main driver for the production of all the chemical species required for these multiple reactions. Curvature Effects and their Interactions. The role of X_1 in COD removal is also more critical because it exhibits nonlinear effects that are not observed for turbidity.
- Quadratic effect (X_{12}): For COD, the term X_1^2 was statistically significant (p=0.036), indicating that there was a precise optimal current point beyond which the efficiency changed. This effect was negligible for turbidity (p=0.360).
- Multiple interactions: For COD, X_1 interactd significantly with time (X_1X_3) and agitation (X_1X_4, p=0.025). These complex interactions make COD yield much more dependent on precise current intensity settings. If current is the dominant factor in both cases, it is the true pivot of COD treatment because it orchestrates more diverse and sensitive chemical reactions than simple water clarification (i.e., turbidity).

This statistical distinction reflects the complexity of the physical phenomena described in the sources.

- Turbidity is removed through a direct coagulation-flocculation mechanism: the more coagulant ions are produced (via current and time), the more particles are trapped (Okolo et al., 2021).
- COD involves more sensitive mechanisms, such as adsorption and oxidation. These processes are not purely proportional ; for example, excessive agitation can break up organic flocs, or too high an intensity can trigger secondary reactions. It is this complexity that creates the "curve" (the quadratic effect) captured by the mathematical model (Sanou et al., 2017).

Comparative Analysis of Turbidity and COD

Turbidity is primarily governed by a relatively simple coagulation-flocculation mechanism, witch explains the absence of marked curvature. In contrast, COD depends on more complex mechanisms (adsorption, oxidation, coprecipitation), which explains the presence of an internal optimum and the significance of the quadratic terms (Assaad et al.,2007).

3.6. Mathematical Modeling: Regression Equations

The final equations in non-coded units are as follows: The terms in bold correspond to factors with a statistically significant impact ($p < 0.05$).

Regression equation for Y_1 (%) is as follows:

$$Y_1(\%) = 88.75 + 2.45\ X_1 - 0.00277\ X_2 - 0.0785\ X_3 - 0.00563\ X_4 + 2.30\ X_1^2 + 0.0000203\ X_2^2 + 0.000330\ X_3^2 + 0.00000968\ X_4^2 + 0.00171\ X_1{*}X_2 + {*}0.1357\ X_1X_3 - 0.00471\ X_1{*}X_4 + 0.0001189\ X_2{*}X_3 + 0.0000130\ X_2{*}X_4 + 0.0000958\ X_3{*}X_4 \quad (8)$$

Regression equation for Y_2 (%) is as follows:

$$Y_2(\%) = 82.44 + 4.49\ X_1 + 0.00154\ X_2 - 0.0631\ X_3 - 0.00047\ X_4 + 3.13\ X_1^2 + 0.00002435\ X_2^2 + 0.000553\ X_3^2 + 0.00001070\ X_4^2 + 0.00614\ X_1{*}_X2 + 0.1064\ X_1{*}X_3 - 0.00789\ X_1{*}X_4 + 0.0000606\ X_2{*}X_3 + 0.00000442\ X_2{*}X_4 + 0.0000521\ X_3{*}X_4 \quad (9)$$

3.7.1. Turbidity optimization:

The contour plot relating X_1 and X_3 illustrates the following points:

Linear behavior: Since the quadratic terms are not significant (p=0.375), the contour lines tend to be relatively straight or exhibit very slight curvature. This indicates that the yield increases steadily and proportionally as the current and time increase.

The significant interaction (p=0.003) between these two factors indicates that to maximize turbidity removal, both parameters must be adjusted simultaneously. The higher the current, the faster the production of coagulating agents, and a longer time allows for the maturation of the flocs, which

The significant interaction (p=0.003) between these two factors indicates that maximizing turbidity removal requires simultaneous adjustment of both parameters. A higher current accelerates the production of coagulating agents, while a longer duration allows flocs to mature, which is graphically represented by peak efficiency zones located in the upper right corner of the graph.

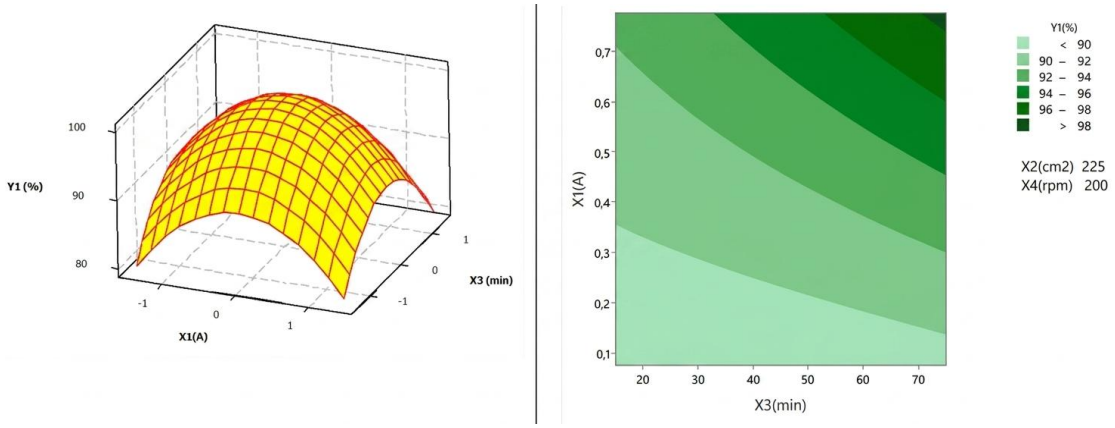


Figure 4: Turbidity variation for X_2: 225 cm² and X_4: 200 rpm.

The multi-objective optimization of the two response functions aims to maximize the process performance. To graphically represent 3-D response surfaces based on the polynomial design of electrocoagulation efficiency, it would be necessary to modify the yield function with respect to only two factors, while fixing the other two variables to a value near the region where the possibility of achieving an optimum is highest.

Therefore, the turbidity yield equation will take the form:

$$Y_1 = 91.81 - 0.075X_1 + 0.0044X_3 + 2.30X_1^2 + 0.000330X_3^2 + 0.1357X_1X_3 \qquad (10)$$

The graph illustrating this equation was created using Minitab software (Figure 4). The plot indicates a maximum yield within the measurement limits of X_1 and X_3, near the optimal value.

3.7.2. Optimization of COD

The contour plots for COD are more complex due to the presence of an internal optimum.

Presence of Curvature (Quadratic Effects): Unlike turbidity, the contour lines for COD exhibit more elliptical or circular shapes. This reflects the fact that the squared terms (X_i^2) are highly significant (p=0.004), indicating that there is a performance peak beyond which efficiency begins to stagnate or decline.

Current-Time Interaction (X_1X_3)

The graph shows a very strong interaction (p=0.000). The maximum yield zone (the contour's "target") is clearly defined by a precise combination of high current and sufficient time to allow for the adsorption and oxidation of organic matter.

The contour plots for COD are more complex due to the presence of an internal optimum.

Presence of curvature (quadratic effects): Unlike turbidity, the contour lines for COD exhibit more elliptical or circular shapes. This indicates that the squared terms (Xi^2) are highly significant (p=0.004), proving that there is a performance peak beyond which efficiency begins to stagnate or decrease.

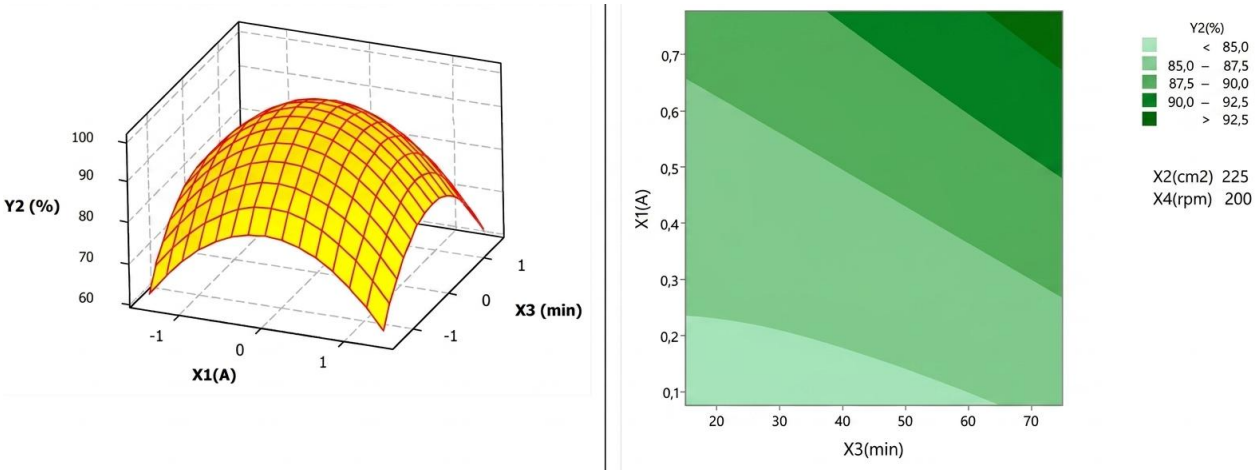


Figure 5: Variation in COD for X_2:225 cm² and X_4:200 rpm.

In order to calculate the maximum DCO yield, the normalized average values for surface area and agitation will be estimated as 225 cm² and 200 rpm, respectively. Therefore, the DCO yield equation will take the following form:

$$Y_2 = 86.41 + 1.03X_1 - 0.019X_3 + 3.13X_1^2 + 0.000553X_3^2 + 0.1064X^1X_3 \quad (11)$$

The graph illustrating this equation was created using Minitab software (Figure 5). The plot indicates a maximum yield within the boundaries of the X_1 and X_3 measurements near the optimal value.

Current–Agitation Interaction (X_1X_4): This graph is critical as it shows a significant interaction (p=0.025). The contour lines reveal that moderate agitation promotes mass transfer, but excessive agitation (too high a speed) combined with high current can break up organic flocs (fragmentation), leading to a drop in yield, visible through a change in the direction of the contour lines.

The contour plots confirm that turbidity follows a straightforward clarification process, while COD requires fine-tuning to achieve an optimal balance between chemical production and the physical stability of the flocs.

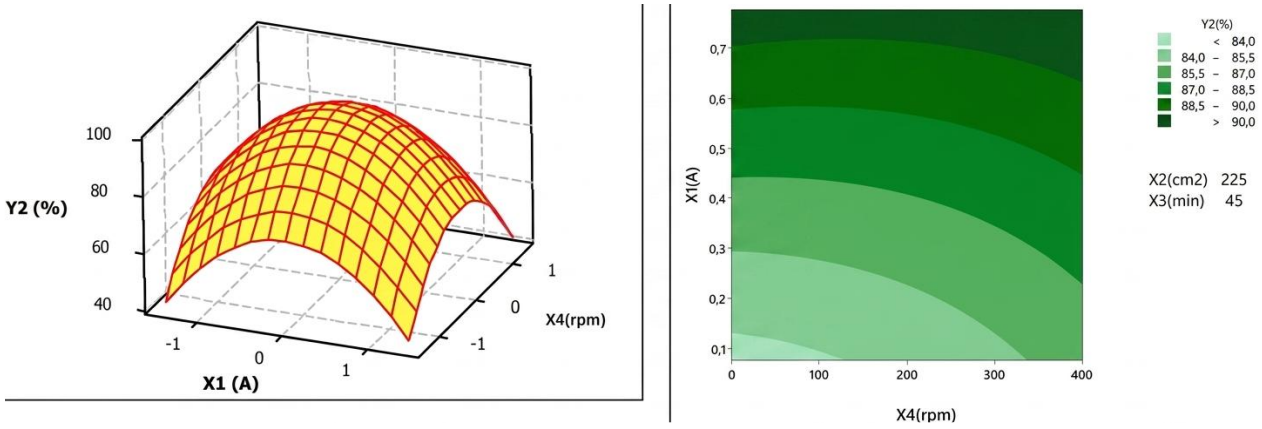


Figure 6: Variation of COD for X_2: 225 cm² and X_3: 45 min.

To calculate the maximum DCO yield, the standardized average values for surface area and time will be estimated as 225 cm² and 45 min, respectively. Therefore, the DCO yield equation will take the following form:

$$Y_2 = 86.52 + 10.17X_1 + 0.0051X_4 + 3.13X_1^2 + 0.00001070X_4^2 - 0.00789X_1X_4 \quad (12)$$

The graph illustrating this equation was created using Minitab software (Figure 6). The diagram indicates a maximum yield between the limits of the X_1 and X_4 measurements, near the optimal value.

According to the statistical optimization results presented in the sources, the optimal operating conditions for maximizing turbidity removal efficiency (Y_1) are identical to those selected for COD in a multi-objective optimization framework:

- Current intensity (X_1): 0.775 A.

- Electrode surface area (X_2): 375 cm².

- Electrolysis time (X_3): 75 min.

- Stirring speed (X_4): 400 rpm.

Under these conditions, the mathematical model predicts an adjusted turbidity efficiency of 103.21%. Although this theoretical value exceeds 100% due to approximations in the statistical model, it indicates nearly complete removal of suspended solids.

For the COD:

According to the results of the multi-objective optimization presented in the sources, the optimal conditions to maximize the COD removal efficiency (Y_2) are as follows:

- Current intensity (X_1): 0.775 A.
- Electrode surface area (X_2): 375 cm².

- Electrolysis time (X_3): 75 min.
- Stirring speed (X_4): 400 rpm.

Under these specific conditions, the model predicts a COD removal efficiency of 97.57%.

This configuration is considered optimal because it accounts for the complexity of COD mechanisms (adsorption, oxidation), which, unlike turbidity, exhibit significant quadratic effects indicating the existence of an internal optimum. For example, stirring (X_4) must be set at this level to promote mass transfer without causing floc fragmentation, which would reduce removal efficiency.

4.Recommendation

The findings of this work demonstrate that optimized electrocoagulation is an efficient, chemical-free technology for removing diverse pollutants from urban wastewater. To support future scale-up and industrial application, subsequent research should focus on:

- ❖ Evaluating the long-term effects of electrode passivation and developing automated electrochemical polarity-reversal schedules to maintain low polarization potentials.
- ❖ Assessing the economic and technical feasibility of coupling electrocoagulation with advanced oxidation processes (e.g., peroxi-coagulation or solar photo-electro-Fenton) to degrade highly recalcitrant organic micro-pollutants.
- ❖ Testing novel multi-element alloy anodes to optimize coagulant generation rates, minimize specific electrical energy consumption, and extend electrode operating lifespans.

5. Conclusion

This study has demonstrated the effectiveness of the electrocoagulation process for treating urban wastewater, using a rigorous optimization approach through response surface methodology combined with a central composite design. The application of this statistical tool proved successful in modeling and predicting treatment performance with high accuracy, as evidenced by the high coefficients of determination (R^2 of 97.72% for turbidity and 99.25% for COD).

Analysis of variance identified current intensity as the most influential parameter on treatment efficiency. However, the study revealed greater complexity in the removal of COD, characterized by significant quadratic effects indicating the existence of an internal optimum linked to adsorption and oxidation mechanisms. In contrast, turbidity reduction followed a nearly linear behavior, primarily governed by the production of coagulating agents.

Multi-objective optimization enabled the determination of ideal operating conditions to simultaneously maximize both efficiencies:

- Current intensity : 0.775 A
- Electrode surface area : 375 cm^2
- Electrolysis time : 75 min
- Stirring speed : 400 rpm

Under these optimal conditions, the process achieves near-total turbidity removal (~100%) and a remarkable 97.57% reduction in COD. These results confirm that electrocoagulation, when optimized by RSM, represents a high-performance and viable technological alternative for treating domestic effluents, offering promising prospects for industrial-scale application while minimizing the use of chemical reagents.

Funding

This study received no external finding. The research was conducted using the facilities of the Materials Engineering and Industrial Analysis Laboratory (M.E.I.A.L.), University of 8 May 1945 Guelma, Algeria.

References

1. Yusmaini, N. A., Suzaimi, N. D., Abuhabib, A., Almanassra, I. W., Bagastyo, A. Y., Adnan, F. H., ... & Hamzah, S. (2026). Electrocoagulation strategies for oily wastewater treatment: a review on process efficiency and optimization. International Journal of Environmental Science and Technology, 23(3), 227. https://doi.org/10.1007/s13762-025-06847-x
2. Mokhter, M. A. (2017). Modification de membranes par des films polymères : application à la décontamination de solutions aqueuses contenant des ions métalliques. Doctoral dissertation. University Bourgogne Franche-Comté.
3. Osman, Y. B. (2022). Traitement électrochimique des eaux usées chargées en polluants émergents utilisant des anodes innovantes à coût maîtrisé. Doctoral dissertation. University Haute Alsace-Mulhouse. Université de Carthage (Tunisie).
4. Natchia, A. K. A., Abou, T., Paul, D. N., & Albert, G. Y. D. (2023). Suivi de la turbidité et des matières en suspension dans les rivières côtières en milieu tropical : cas de la Mé et de l'Agneby (sud-est de la Côte d'Ivoire). Journal of Applied Biosciences, 183, 19103-19122. https://doi.org/10.35759/jabs.183.1
5. Nabbou, N., Benyagoub, E., Bekaddour, M., Larabi, B., & Hamouine, A. (2025). Removal of organic matter, phosphates, and nitrates present in pond wastewater using chemical coagulant solutions. BMC chemistry, 19(1), 278. https://doi.org/10.1186/s13065-025-01642-8
6. Bellebia, S., Kacha, S., Bouberka, Z., Bouyakoub, A. Z., & Derriche, Z. (2009). Color removal from acid and reactive dye solutions by electrocoagulation and electrocoagulation/adsorption processes. Water Environment Research, 81(4), 382-393. https://doi.org/10.2175/106143008X357200
7. Shamshad, J., & Rehman, R. U. (2025). Innovative approaches to sustainable wastewater treatment: a comprehensive exploration of conventional and emerging technologies. Environmental Science : Advances, 4(2), 189-222. https://doi.org/10.1039/d4va00136b
8. Zodi, S. (2012). Étude de l'épuration d'effluents de composition complexe par électrocoagulation et des couplages intervenants entre le traitement électrochimique et l'étape de séparation : application à l'industrie textile et papetière. Doctoral dissertation, 196.
9. García-Segura, S., Eiband, M. M. S., de Melo, J. V., & Martínez-Huitle, C. A. (2017). Electrocoagulation and advanced electrocoagulation processes: A general review about the fundamentals, emerging applications, and their association with other technologies. Journal of Electroanalytical Chemistry, 801, 267-299. https://doi.org/10.1016/j.jelechem.2017.07.047

10. Al-Shannag, M., Al-Qodah, Z., Bani-Melhem, K., Qtaishat, M. R., & Alkasrawi, M. (2015). Heavy metal ions removal from metal plating wastewater using electrocoagulation: Kinetic study and process performance. Chemical Engineering Journal, 260, 749-756. https://doi.org/10.1016/j.cej.2014.09.035

11. Bazrafshan, E., Mohammadi, L., Ansari-Moghaddam, A., & Mahvi, A. H. (2015). Heavy metals removal from aqueous environments by electrocoagulation process–a systematic review. Journal of environmental Health Science and Engineering, 13(1), 74. https://doi.org/10.1186/s40201-015-0233-8

12. Bayramoglu, M., Kobya, M., Can, O. T., & Sozbir, M. (2004). Operating cost analysis of electrocoagulation of textile dye wastewater. Separation and Purification Technology, 37(2), 117-125. https://doi.org/10.1016/j.seppur.2003.09.002

13. Núñez, J., Yeber, M., Cisternas, N., Thibaut, R., Medina, P., & Carrasco, C. (2019). Application of electrocoagulation for the efficient removal of pollutants to reuse the treated wastewater in the dyeing process of the textile industry. Journal of Hazardous Materials, 371, 705-711. https://doi.org/10.1016/j.jhazmat.2019.03.030

14. Zongo, I. (2009). Étude expérimentale et théorique du procédé d'électrocoagulation : application au traitement de deux effluents textiles et d'un effluent simulé de tannerie. Doctoral dissertation. Institut National Polytechnique. Lorraine

15. İrdemez, Ş., Yildiz, Y. Ş., & Tosunoğlu, V. (2006). Optimization of phosphate removal from wastewater by electrocoagulation with aluminium plate electrodes. Separation and Purification Technology, 52(2), 394-401. https://doi.org/10.1016/j.seppur.2006.05.020

16. Asselin, M. (2007). Utilisation de l'électrocoagulation dans le traitement des eaux usées industrielles chargées en matière organique. Institut National de la Recherche Scientifique (Canada).

17. Li, B., & Wang, Y. (2025). A comparative review of removing chromium (VI) from electroplating industry wastewater using electrocoagulation and membrane filtration. Science and Technology of Engineering, Chemistry and Environmental Protection, 1(3). https://doi.org/10.61173/jnefwt44

18. Adhoum, N., Monser, L., Bellakhal, N., & Belgaied, J. E. (2004). Treatment of electroplating wastewater containing Cu2+, Zn2+ and Cr (VI) by electrocoagulation. Journal of Hazardous Materials, 112(3), 207-213. https://doi.org/10.1016/j.jhazmat.2004.04.018

19. Kamar, F. H., Esgair, K. K., Abod, B. M., & Nechifor, A. C. (2018). Removal of hexavalent chromium ions from the simulated wastewater using electrocoagulation process. SIMI, 111. http://doi.org/10.21698/simi.2018.fp14

20. Moussa, D., El-Naas, M., Nasser, M., & Al-Marri, M. (2017). A comprehensive review of electrocoagulation for water treatment: potentials and challenges. Journal of Environmental Management, 186 Pt 1, 24-41. https://doi.org/10.1016/j.jenvman.2016.10.032

21. Bennajah, M. (2007). Traitement des rejets industriels liquides par électrocoagulation/électroflottation en réacteur airlift (Doctoral dissertation, Institut National Polytechnique (Toulouse)).

22. Fouad, Y. O. A., Konsowa, A. H., Farag, H. A., & Sedahmed, G. H. (2009). Performance of an electrocoagulation cell with horizontally oriented electrodes in oil separation compared to a cell with vertical electrodes. Chemical Engineering Journal, 145(3), 436-440. https://doi.org/10.1016/j.cej.2008.04.027

23. Zaied, B., Rashid, M., Nasrullah, M., Zularisam, A., Pant, D., & Singh, L. (2020). A comprehensive review of contaminant removal from pharmaceutical wastewater by the electrocoagulation process. The Science of the Total Environment, 726, 138095. https://doi.org/10.1016/j.scitotenv.2020.138095.

24. Ebba, M., Asaithambi, P., & Alemayehu, E. (2022). Development of the electrocoagulation process for wastewater treatment: optimization by response surface methodology. Heliyon, 8. https://doi.org/10.1016/j.heliyon.2022.e09383.

25. Asaithambi, P., Beyene, D., Aziz, A. R. A., & Alemayehu, E. (2018). Removal of pollutants with determination of power consumption from landfill leachate wastewater using an electrocoagulation process: optimization using response surface methodology (RSM). Applied Water Science, 8(2), 69. https://doi.org/10.1007/s13201-018-0715-9

26. Dubrawski, K. L., Du, C., & Mohseni, M. (2014). General potential-current model and validation for electrocoagulation. Electrochemical Acta, 129, 187-195. https://doi.org/10.1016/j.electacta.2014.02.089

27. Nasrullah, M., Zularisam, A., Krishnan, S., Sakinah, M., Singh, L., & Fen, Y. (2019). High-performance electrocoagulation process in treating palm oil mill effluent using high current intensity application. Chinese Journal of Chemical Engineering. https://doi.org/10.1016/j.cjche.2018.07.021

28. Wu, T., Han, M., & Xu, Z. (2022). Size Effects of Electrocatalysts: More Than a Variation of Surface Area. ACS Nano. https://doi.org/10.1021/acsnano.2c04603

29. Ibrahim, H., & Salman, R. (2022). Study the Optimization of Petroleum Refinery Wastewater Treatment by Successive Electrocoagulation and Electro-oxidation Systems. Iraqi Journal of Chemical and Petroleum Engineering. https://doi.org/10.31699/ijcpe.2022.1.5

30. Trinh, D., Quach, A., Ty, T., Channei, D., Nakaruk, A., & Khanitchaidecha, W. (2021). Evaluation of Magnetic Stirring and Aeration on Electrocoagulation Performance in Actual Industrial Treatment. https://doi.org/10.3389/fenvs.2021.719248

31. Khemis, M. (2005). Étude théorique et expérimentale du procédé d'électrocoagulation : application au traitement des effluents liquides hautement chargés en impuretés organiques et métalliques (Doctoral dissertation, Institut National Polytechnique de Lorraine)

32. AlJaberi, F. Y. (2023). New design of an electrocoagulation reactor to remove pollutants from groundwater: Analysis and optimization using response surface methodology. South African Journal of Chemical Engineering, 46, 205-216. https://doi.org/10.1016/j.sajce.2023.08.008

33. Bhattacharya, S. (2021). Central Composite Design for Response Surface Methodology and Its Application in Pharmacy. Response Surface Methodology in Engineering Science [Working Title]. https://doi.org/10.5772/intechopen.95835

34. Trigueros, D., Braun, L., & Hinterholz, C. (2022). Environmental and economic feasibility of the treatment of dairy industry wastewater by photo-Fenton and electrocoagulation processes: multicriteria optimization by desirability function. Journal of Photochemistry and Photobiology A: Chemistry. https://doi.org/10.1016/j.jphotochem.2022.113820

35. Mäkelä, M. (2017). Experimental design and response surface methodology in energy applications: A tutorial review. Energy Conversion and Management, 151, 630-640. https://doi.org/10.1016/j.enconman.2017.09.021

36. Talhi, B. (2010). Optimisation de la réduction des nitrates par voie électrochimique (Doctoral dissertation, École de technologie supérieure).

37. Obi, C., Nwabanne, J., Igwegbe, C., Ohale, P., & Okpala, C. (2022). Multi-characteristic optimization and modeling analysis of electrocoagulation treatment of abattoir wastewater using iron electrode pairs. Journal of Water Process Engineering. https://doi.org/10.1016/j.jwpe.2022.103136

38. Mousazadeh, M., Khademi, N., Kabdaşlı, I., Rezaei, S., Hajalifard, Z., Moosakhani, Z., & Hashim, K. (2023). Domestic greywater treatment using the electrocoagulation-electrooxidation

process: optimization and experimental approaches. Scientific Reports. https://doi.org/10.1038/s41598-023-42831-6

39. Okolo, B., Adeyi, O., Oke, E., Agu, C., Nnaji, P., Akatobi, K., & Onukwuli, D. (2021). Coagulation kinetic study and optimization using response surface methodology for effective removal of turbidity from paint wastewater using natural coagulants. Scientific African. https://doi.org/10.1016/j.sciaf.2021.e00959
40. Sanou, Y., Paré, S., Baba, G., Segbeaya, N., & Bonzi-Coulibaly, L. (2017). Removal of COD in wastewaters by activated charcoal from rice husk. Journal of Water Science, 29, 265-277. https://doi.org/10.7202/1038927ar
41. Assaad, E., Azzouz, A., Nistor, D., Ursu, A. V., Sajin, T., Miron, D. N., ... & Hausler, R. (2007). Metal removal through synergic coagulation–flocculation using an optimized chitosan–montmorillonite system. Applied Clay science, 37(3-4), 258-274.

Figures captions

Figure 1: Experimental setup of the EC assembly.

Figure 2: Normalized Effects Pareto Diagram for Response Y1.

Figure 3: Normalized Pareto chart of effects for response Y2.

Figure 4: Turbidity variation for X_2: 225 cm² and X_4: 200 rpm.

Figure 5: Variation in COD for X_2:225 cm² and X_4:200 rpm.

Figure 6: Variation of COD for X_2: 225 cm² and X_3: 45 min.

Tables captions

Table 1: Experimental parameter variation domains and levels studied.

Table 2: Matrice.

Table 3: Wastewater characteristics.

Table 4: Definition of the influencing factors and responses of the experimental design.

Table 5: Regression parameters and determination coefficients for turbidity yield.

Table 6: Analysis of Variance (ANOVA) Results for the Response Surface Model of Turbidity.

Table 7: Regression parameters and coefficients of determination for COD yield.

Table 8: Analysis of Variance (ANOVA) Results for the Response Surface Model of COD.

Supplementary Files

This is a list of supplementary files associated with this preprint. Click to download.

- Table1.docx
- graphicalabstract.pdf
- SarraHamidoudcoverletter2.docx
- Tiltlepage.docx
- Highlights.pdf